Available online www.ejaet.com

European Journal of Advances in Engineering and Technology, 2019, 6(8):1-10

Research Article ISSN: 2394 - 658X

Pulsed Magnetic Fields May Affect the Ultrastructure of Live Bacteria Cells Containing Endogenous Magnetosome Chains

Simona Miclaus[1], Lucian Barbu-Tudoran[2], Cristina Moisescu[3], Laura Darabant[4], Paul Bechet[1], Simona Oancea[5] and Mihaela Racuciu[5]

[1]Department of Technical Sciences,"Nicolae Balcescu" Land Forces Academy, Sibiu, Romania
[2]Institute for R&D for Isotopic and Molecular Technologies, and Babes-Bolyai University, Cluj-Napoca, Romania
[3]Department of Microbiology, Institute of Biology Bucharest, Romanian Academy, Bucharest, Romania
[4]Department of Electrotechnics and Measurements, Technical University of Cluj-Napoca, Romania
[5]Lucian Blaga University, Sibiu, Romania
simo.miclaus@gmail.com

ABSTRACT

A magnetic field applied in trains of pulses or bursts, with an average flux density not exceeding 125 mT and covering the frequency band up to 3.5 MHz was delivered to liquid suspensions of bacteria Magnetospirillum gryphiswaldense cells with the aim of observing field-induced effects on internal magnetosome chains. Scanning-transmission electron microscopy and Fourier Transform Infrared Spectroscopy revealed mild ultrastructural changes and possible proteins damaging.

Key words: Magnetotactic bacteria, magnetosome chains, transcranial magnetic stimulation, figure of eight coil, magnetic pulses

---

INTRODUCTION

Natural magnetite (Fe_3O_4) nanoparticles are produced by a limited number of organisms including magnetotactic bacteria (MTB) – which biomineralize them in the form of chained magnetosomes (MS). Generally, ferri- and ferromagnetic synthetic nanoparticles have today many important applications in medicine and biotechnology but the use of biogenic magnetic nanoparticles is of more recent data [1]. Knowledge about MS formation, influences, role and responses to various stimuli is still sprinkled with gaps.

MS are in fact bacteria organelles used primarily for sensing and navigating in the geomagnetic field. A MS is a vesicle that contains a ferrimagnetic nanoparticle (magnetite or greigite) enveloped in a membrane consisting of lipids and proteins. In MTB the MS are not encountered as individuals but as chains of usually tens of vesicles. MS formation is controlled by a set of MS-associated proteins that influence the magnetism of MTB and they are grouped in magnetosome-associated membrane (Mam) proteins and magnetic particle membrane-specific (Mms) proteins [2]. The form of the MS chain is slightly different for different MTB species but it generally has a strong dynamic character [3].

In the present study we analyzed the magnetotactic bacteria *Magnetospirillum gryphiswaldense* bacterium species which produces MS with average and standard deviation values of the dimensions (39.93±9.23) nm and median dimension of 40.73 nm [4], while the chains usually contain 20-60 vesicles. The bacterium cell shape is helical and the length is between 2-6 µm. The magnetite nanoparticles of this species have a cub-octahedral geometry and the magnetic easy axis [111] is aligned along the chain axis. The electron cryotomogram of a MS chain showed that its form is not a straight line but a helical-shaped line [5]. Due to two antagonistic anisotropies, magnetocrystalline- and shape anisotropy respectively, the effective magnetic moment of an individual MS is tilted out of the crystallographic easy axis of magnetite (chain) by 20°. The tilts do not change the net magnetic moment of the chain (along [111] axis), but conduct to the helical form of the chains. The shape is therefore a result of both the magnetic dipolar interactions between MS (each individual magnetic moment orientation counting) and an elastic recovery force exerted on the MS provided by the lipid/protein which sustain the mechanism. The magnetite crystals in the MS are single-domain nanoparticles and their magnetization is also oriented parallel with each others in the chain. Practically a large magnetic

dipole is formed in this way inside each bacterium cell. Therefore, an external magnetic field could be able to modify the MS structures (reversible or irreversible) – and this may happen either during formation of chains or after they are already formed [6]. Magnetic moment of MS belonging to *Magnetospirillum gryphiswaldense* were measured and a recent work [7] mentions that the bacteria cells present an average saturation magnetic moment μ_{sat_avg} = (9.9±2.6)x10^{-16} A.m^2, a maximal saturation magnetic moment μ_{sat_max} = 16.7x10^{-16} A.m^2 and a minimal one μ_{sat_min} = 4.9x10^{-16} A.m^2. With this data we could estimate both the force F (translation) and the torque τ (rotation) produced by a magnetic field on a MTB cell. External magnetic fields, either static or alternative, have been clearly demonstrated to affect the MS chains of MTB [6], [8]. When applied as pulses, the responses to such stimuli and the mechanisms underlying the response have been scarcely investigated yet [9], [10]. Present work aimed to quantify the response of whole MTB cells (in liquid suspension) to pulsed magnetic field (PMF) by means of electron microscopy analysis and by Fourier Transform Infrared Spectroscopy (FTIR).

Investigations of the response of MTB suspensions to static magnetic fields showed that MS size, morphology and rate of production is affected [6]. When MTB was entrapped in an agarose hydrogel matrix (for restriction of whole cell rotation), re-orientation and changes as significant as destructuring of MS chains were observed [8]. Chains ruptures installed at a field flux density of 35 mT and they proved to be reversible (recovered chains) if the MTB cells didn't suffer a prior cell chemical fixation. The biological equivalent force in vivo was calculated to be of 25 pN. The broken chain recovery could be explained by considering that the assembly of proteins responsible of nanocrystals organization (chain integrity) has a strong dynamic character. From a newer study [6] that reported similar but also dissimilar effects of static magnetic fields, emerged two possible mechanisms of interaction: a) each MS may respond individually and reorients in the field direction; b) short MS chains deviate in the magnetic field direction. The chain deviation could be reversible at field turned-off, probably because the assembly has an elastic character. The effect of chain re-orientation on cell viability and its impact on the crystallographic and magnetic orientation of the nanoparticles are still under investigation. The effect of static magnetic field on MS chains was theoretically modelled also. Authors of [3] proved by Monte Carlo numerical simulation that a MS change of position or reorientation not only saves elastic energy but conducts to a structural rearrangement of electrons in lipids, proteins, etc. This appears because a very high gradient of magnetic field is generated in the immediate vicinity of the single-domain magnetite crystal. In this way MS chain also represents a store of elastic energy.

First experiments with pulsed magnetic fields (PMF) were made back in 1991 with the aim of separating bacteria cells on the basis of their magnetic coercivities [11]. Cultures of *Aquaspirillum magnetotacticum* in the exponential growth phase were investigated and a maximum bulk coercivity of 40 mT was obtained after a treatment with a 55 mT pulse. With higher magnetic field levels the authors reported not an increased coercivity but an increase of magnetostatic interactions of MS chains, an increase of cell percentage showing abnormal distributions of MS chains and appearance of cystlike cells empty of MS chain. Abnormal MS chains appearance when larger field strength pulses were applied conducted to the hypothesis that MS collapsed due to strong inter-particle magnetic interactions. Later in 2009, investigating pulsed magnetic field of only 1 mT effect on growth and MS formation in *Magnetospirillum magneticum* AMB-1, it was observed that growth of cells was not affected but: the number of MS containing cells increased; the formed chains were longer and with more heterogeneous nanocrystal dimensions distribution; the magnetite's precipitation was affected [10]. The authors hypothesized that the PMF upregulated some proteins (magA and MamA) expression in cells. Convergent results with that ones where obtained in 2010 with a 50 Hz, 2 mT pulsed magnetic field applied on *Magnetospirillum sp.* strain AMB-1 during the development of the bacteria. The stimuli significantly enhanced cellular magnetism while the cells growth was not affected by the exposure. The average number of MS per cell increased by 15% while very small and very large MS have been formed due to the exposure. Lower strength of PMF had no significant effect on the bacterial cell morphologies but still the crystallization process was slightly affected [9].

High intensity PMF (hundreds of mT) is produced by coil-probes used in transcranial magnetic stimulation (TMS) of the brain [12]. Biological material containing magnetic nanoparticles (including brain) may respond to such fields in ways insufficiently explored [13]. A significant heating effect was recently reported in magnetite nanoparticles distributed in agarose gel exposed to 1000 biphasic pulses at 60 Hz delivered by a TMS coil [14]. Literature indicates however that magnetothermal control of neural activity installs if the field is in the frequency range (100 kHz - 1 MHz) [15] while magnetic hyperthermia is generally used in the (100-500) kHz range [1]. It is worth mentioning that PMF delivered by TMS coils to biological material which didn't contain magnetic nanoparticles induced a set of effects: a) molecular uptake of cells [16]; b) neural cells were affected [12]; c) brain stimulation thresholds exist and they could be calculated [17].

In such circumstances, the present work aimed at revealing PMF effect specificities, if delivered in pulse trains or in bursts, on the ultrastructure and molecular aggregate of MTB liquid suspensions.

MATERIALS AND METHODS

Liquid Suspensions of Magnetotactic Bacteria

Magnetospirillum gryphiswaldense bacteria (Fig. 1a) were purchased from the Leibniz DSMZ-German Collection of Microorganisms and Cell Cultures (DSM-6361). Cells were grown under microaerobic conditions, in a flask standard

medium [18]. Cells were harvested when they reached the stationary growth phase by centrifugation at 7000 rpm for 10 min. The supernatant (spent growth medium) was discarded, and the cell pellet was resuspended in fresh culture medium to a concentration of 1.96×10^9 cells/ml (determined spectrophotometrically using a calibration curve of optical density OD565 versus direct cell counts). This bacterial suspension was used in all subsequent experiments. Sample volumes of either 8 ml (first series of experiments) or 2 ml (second series of experiments) were separated and prepared for PMF exposures with different parameters. Bacterial cells contained naturally-formed inner chains of MS with an average diameter ≈ 40 nm and with lengths ranging between 2 – 5 μm (Fig. 1b).

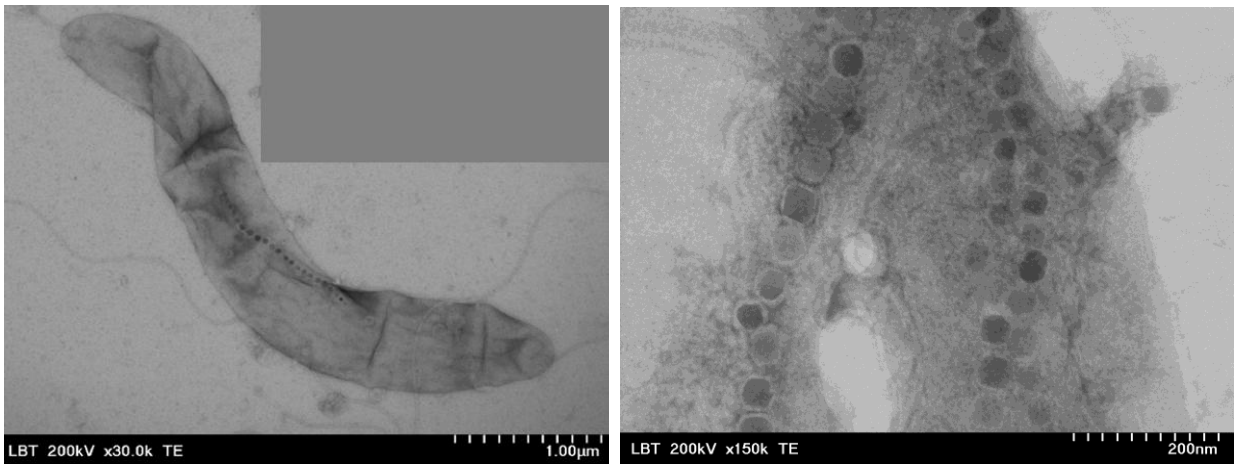

(a) (b)

Fig. 1 a. Scanning-transmission electron microscopy image of a single bacterial cell of *Magnetospirillum gryphiswaldense* with the inner chain of magnetosomes visible; b. Zoomed image of chains of magnetosomes revealing the cub-octahedral shape of magnetite nanocrystals enveloped in the thin membranes of lipids and proteins (left side of image b)

Pulsed Magnetic Field Stimuli Application and Characterization

PMFs (time varying short pulses of magnetic field) were generated by a Magstim Rapid 2 equipment enabled with a D70 Alpha coil model („figure of eight" / double coil shape, Fig. 2a). The average inductance of the coil was 16μH, the coil diameter was 2 x Ø70 mm and peak magnetic field could reach 0.92 T at the surface of the coil. Measurements have shown that at 5 mm distance from this type of coil, the maximum axial flux density over the area of one loop was 0.69 T – which is equivalent to a magnetic field strength (H) of 550 kA/m [12] while at the extremities of the coil (including limits between the tandem coils) the field decreased abruptly, to 100 kA/m. The supplied current in the double coil is a pulsed one with the magnitude of 5 kA at a frequency of 2.5 kHz (pulse duration is T=400 μs). Practically, in the two loops of the coil, one pulse of current with amplitude of 5 kA circles in clockwise and counter-clockwise directions respectively. So each loop will produce a time varying magnetic field changing from 0 to its peak value during its first half period, in opposite directions one to another and then the supplied current in both coils will change from its peak of 5 kA to 0 during the second half period. Therefore, the difference between the areas over each of the loop is the sequence of the magnetic field vectors orientation. The samples of bacteria cell suspension were positioned for exposure as shown in Fig. 2b/2c, in positions where the magnetic flux density was, on average, lower than 125 mT. Positioning as in Fig. 2b provided a more heterogeneous exposure than positioning as in Fig. 2c due to axis orientation of the sample with respect to the axes of the two coils. The two different orientations of the samples were used in the two different repetitions of exposures to the same PMF stimuli.

(a) (b)

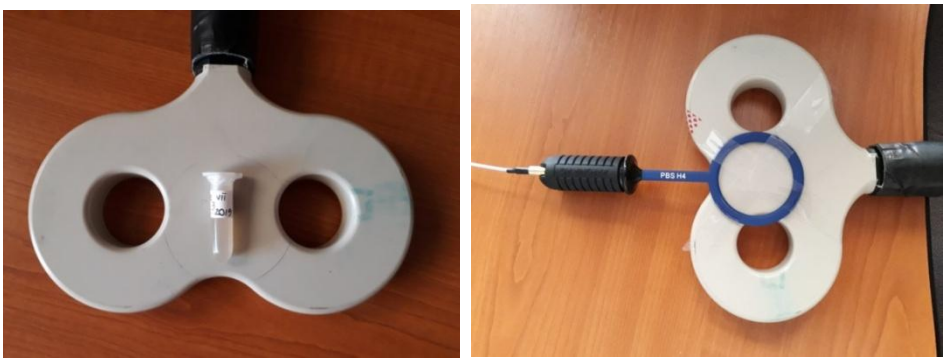

(c) (d)

Fig. 2 a. Magstim Rapid 2 equipment with D70 Alpha coil connected for PMF exposures; b & c. Bacteria suspension samples positioned for exposures; d. H field probe positioned for the characterization of the applied magnetic stimuli

Table -1 Magnetic Stimuli Characteristics of the PMF Used for MTB Exposures

Magnetic stimulus notation	Stimulus type	Power (%)	Frequency (Hz)	Duration (s)	Number of pulses	Wait time (s)	Number of trains	Number of bursts	Cycle time (s)	Burst frequency (Hz)	Number of cycles	Total number of pulses
S1	Trains of pulses	100	10	2	20	2.7	5	-	-	-	-	100
S2	Bursts	80	15	-	10	-	-	3	3	1	10	300
S3	Bursts	90	15	-	3	-	-	10	8	4	10	300

Three types of PMF (stimuli) were applied in each of the two series of experimental repetitions, each type being applied twice repeatedly on the same sample. The samples were analyzed after PMF treatments for expected effects and the results were compared against a not-exposed sample (control). In Table 1 the parameters of the PMF stimuli (denoted with S1 to S3) are presented. Overall we used one stimulus of the type standard repetitive stimulation / pulse trains (S1) and two types of burst of pulses repeated in cycles (S2 and S3). Samples of MTB suspensions numbered P1 and P2 were exposed to stimulus S1, samples P4 and P5 were exposed to stimulus S2 and samples P6 and P7 were exposed to stimulus S3. Sample P3 was not considered, since its exposure was unfinished due to overheating of the coils during the exposure session. In Table 1, column denoted as "Power (%)" refers to the percentage of power delivered by the coil: 100% power means that a peak of 5 kA current circulates in the coils while 90% power means a reduction of the current and of produced magnetic field strength H at 94.8 % (square root of power).

The spectral analysis of the magnetic field component in air (the component perpendicular to the coil surface) for each stimulus was made by capturing the field with a magnetic field probe PBS-H4 from Aaronia A.G. (Fig. 2d) and analysed by a Picoscope 3000 oscilloscope and by a Universal Software Radio Peripheral (USRP) platform enabled with dedicated software.

Instruments and Methods to Investigate the Effects

Scanning-transmission electron microscopy (STEM) of all exposed samples and of controls was applied, with the aim of observing structural changes / mechanic damage of cells due to magnetite nanoparticles displacement. A cold field emission gun STEM microscope Hitachi SU8230, 30 kV, was used. Fourier Transform InfraRed (FTIR) spectroscopy was applied with the aim of identifying variations in the total composition of the cells through the assessment of changes in functional groups of biomolecules. Practically, the vibration and rotation of molecules is traced when an infrared radiation at a specific wavelength is sent to the sample. Structural changes in the molecular binding between microorganisms and metal atoms were successfully observed by this technique [19] and magnetic field treatment of wheat seedlings revealed that structural variation of lipids could be emphasized, rather than that of proteins, by this approach [20]. FTIR spectra of purified and sterilized magnetosomes extracted from *Magnetospirillum gryphiswaldense* have been previously obtained by authors of [21] showing five characteristic peaks at 3273, 2921, 1735, 1645 and 1531 cm^{-1}. Similar spectra of MS were reported in [22], while the spectra of magnetite are presented in [23]. Present spectra of MTB suspensions were obtained by using an Alpha ATR-FTIR Spectrometer - Bruker Optics (with ZnSe crystal, scanning range = 600–4000 cm^{-1}, resolution = 4 cm^{-1}).

In the first series of experiments, the cells were investigated few hours after finalizing all exposures, without taking into consideration the delays between each sample's exposure start and without fixing the cells. In the second series of experiments, glutaraldehyde was used as a chemical fixative of the cells immediately after the exposure (to preserve the intracellular organization when the stimulus was turned off). Different effects of static magnetic fields at around 35 mT have been observed when MTB cells were investigated with and without chemical fixation by paraformaldehyde [6], so that we also expected some differences.

It is important to underline here the fact that, during the first series of exposures, the sample had a larger volume which could be spread on a larger area nearby the double coil, this volume being traversed by a much larger variation of

magnetic field strengths (Fig. 2b). At repetition of the exposures in the second series we used both smaller volumes of the samples (meaning a restricted spread in space, i.e. less variation of field strength with position) and a different position of the sample (Fig. 2c) which enabled in fact a much lower average H-field strength incident to the sample. In consequence, the second set of exposures, which conducted to no effects revealed by our analyses, will not be presented further on in the Results section.

RESULTS AND DISCUSSION

Amplitude-Time-Frequency Analysis of the Applied Magnetic Pulse Trains and Bursts

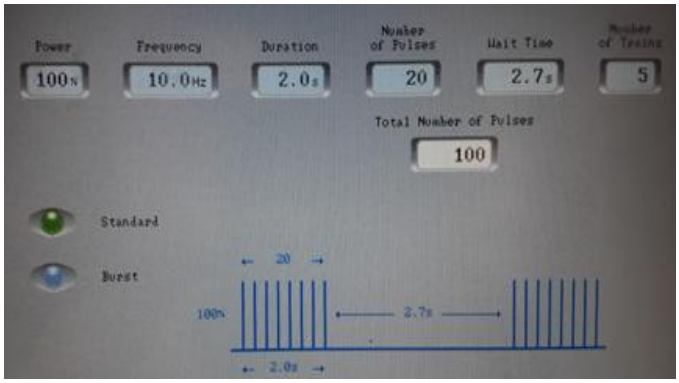

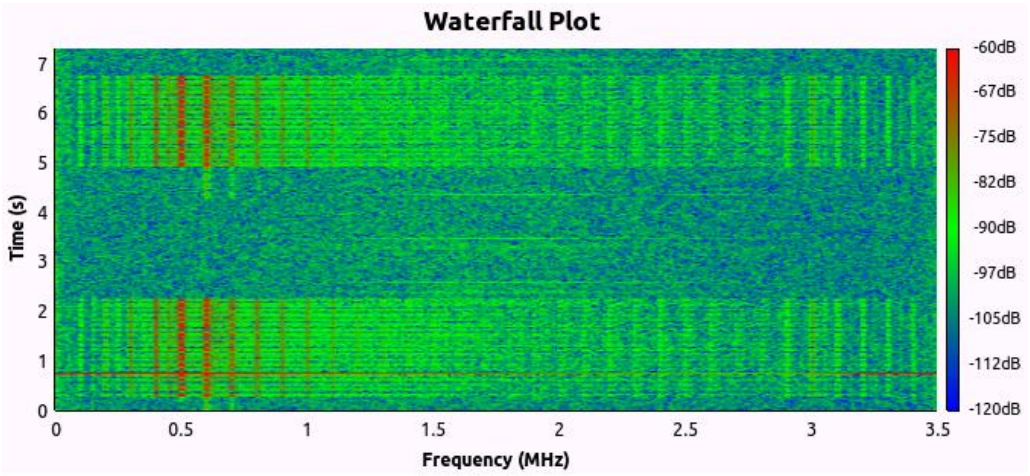

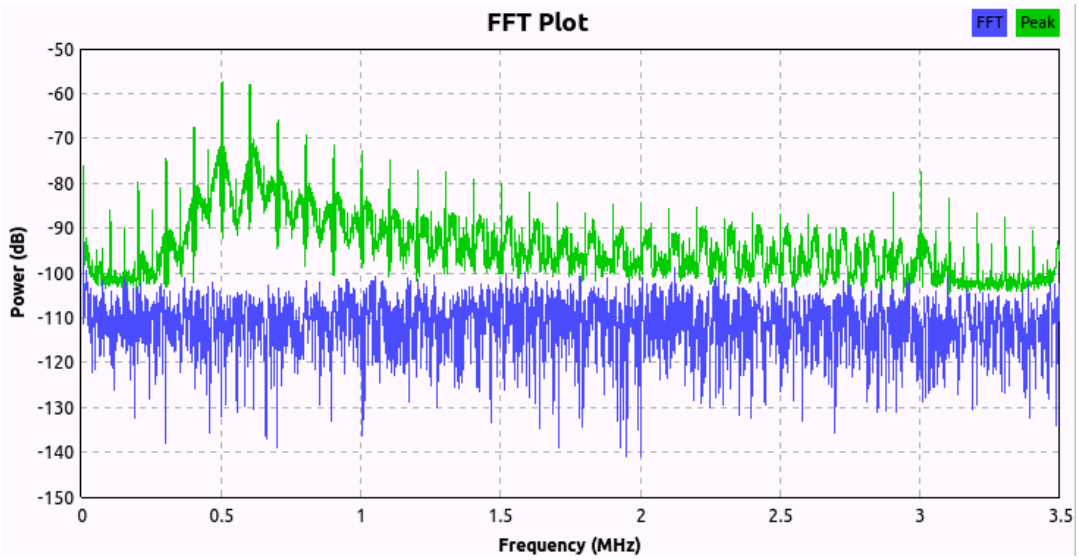

Fig. 3 a. PMF applied as stimulus S1 – parameters set for the pulse trains; b. Recovered spectrogram – waterfall plot of frequency-time distribution of the field strength of stimulus S1; c. Fast Fourier Transform of the stimulus S1 to observe the frequency components of the pulse train

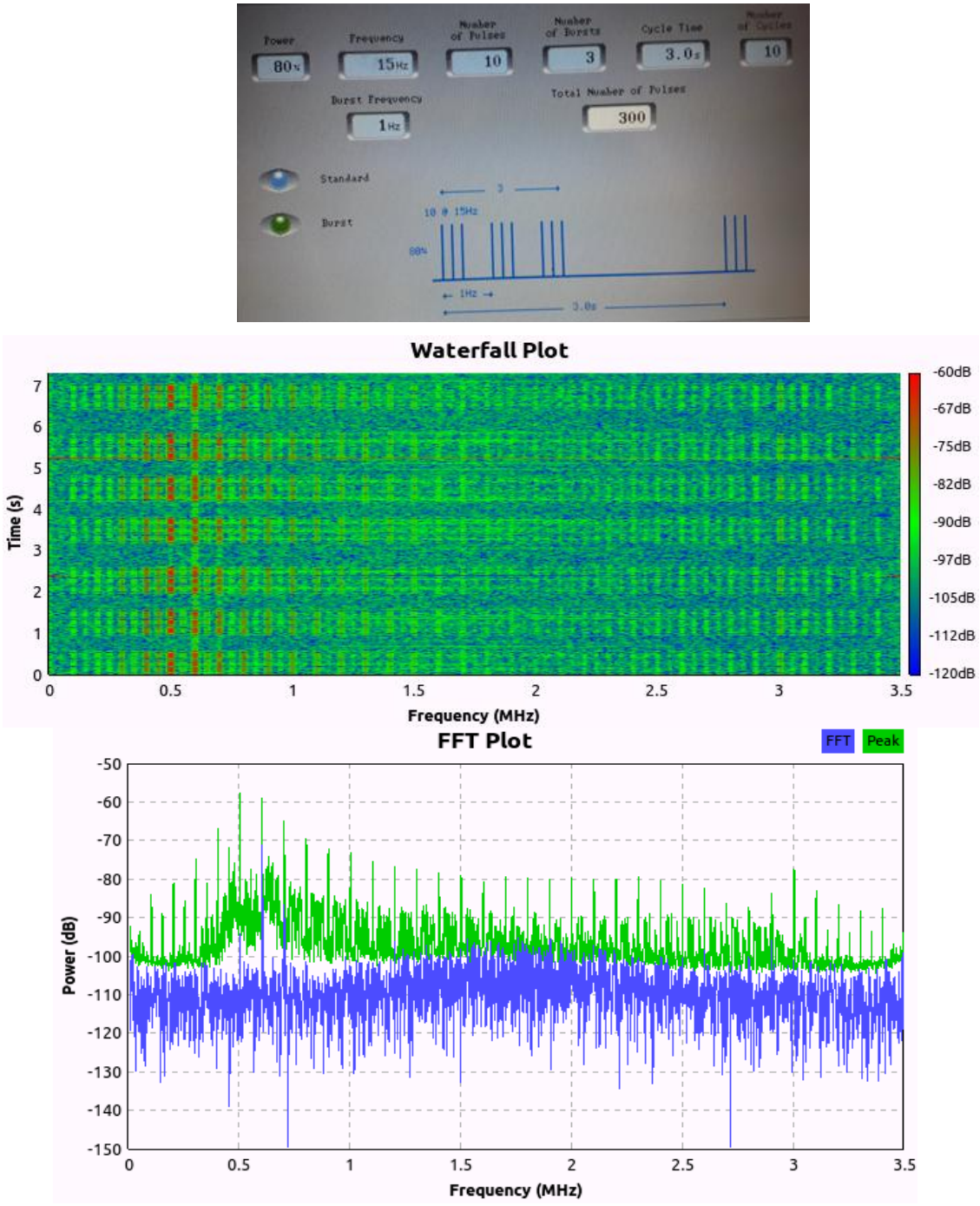

Fig. 4 a. PMF applied as stimulus S2 – parameters set for the bursts; b. Recovered spectrogram – waterfall plot of frequency-time distribution of the field strength of stimulus S2; c. Fast Fourier Transform of the stimulus S2 to observe the frequency components of the burst

Stimuli S1 (trains of pulses) and S2 (burst of pulses) are analyzed separately in Fig. 3 and Fig. 4 respectively. In each figure, the first representation (a) is the display of the Magstim Rapid 2 - for practical parameters observation. Representations (b) and (c) show the processed data acquired from the H-field probe. Fig. 3b shows the spectrogram of two out of a total of five trains of pulses, each of them containing 20 pulses. As observed, a bandwidth of 3.5 MHz is covered, and most importantly, some differences / imperfections in each pulse repetition are seen from one train to another. The same is true for Fig. 4b, where one observes that the bursts are not really identical inside the cycles. Fig. 3c and Fig. 4c show the spectrum of the stimuli, to observe the amplitude-frequency distribution obtained by Fast Fourier Transform (FFT) of the captured magnetic signal. The green print is the peak hold of the spectrum, while the blue print is the momentary spectrum. While the frequency band remains practically the same for all three stimuli, both the spectral content and the time-amplitude representations ("Waterfall") emphasize the differences which were expected to be reflected in the effects on the MTB cell suspensions.

Electron Microscopy Images of the Exposed Magnetotactic Bacteria Cells

With a reduced frequency, but still observed in the PMF exposed samples, some differences between control (Fig. 5a) and treated samples (Fig. 5 b-h) were revealed. The significant effects observed on the micrographs are shown in Fig. 5 for the following situations: MS chains bending and curving – (c), (d); MS chains looping – (f); MS chains breaking in smaller chains – (b), (g); cyst-like cells formation – (b), (d), (f); coccoid cells empty of chains - (b), (c), (d), (h); releasing of MS – (b), (e). The frequency of such events was not high and some of them were also present in the control sample (Fig. 5a). However, observing large microscopic fields conducted to the conclusion that both pulse trains and pulse bursts were able to affect the cellular ultrastructure and no specificities could be assigned to the three types of stimuli. Our findings are convergent with the description in [24] for untreated cells case and with reported changes due to field exposure made by the authors of [11]. Since the average magnetic flux density was B = 125 mT in the volume of the samples, we can calculate the average torque applied to a *M. gryphiswaldense* cell, $\tau = 1.24 \times 10^{-16}$ N.m. For this calculation we considered an average saturation magnetic moment $\mu_{sat\_avg} = (9.9 \pm 2.6) \times 10^{-16}$ A.m^2 provided in [7]. A torque of a very similar value, 1×10^{-16} N.m, have been recently reported to act during propulsion of *Eschericha coli* bacteria by its flagella [25].

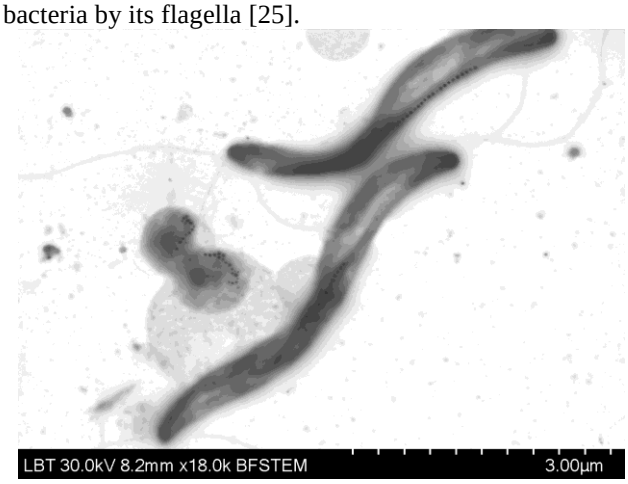

(a)

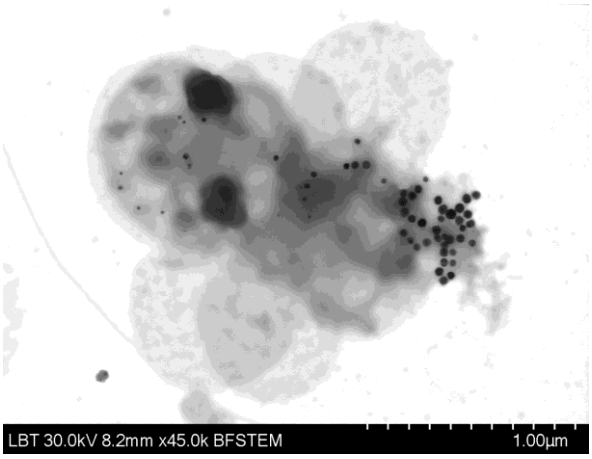

(b)

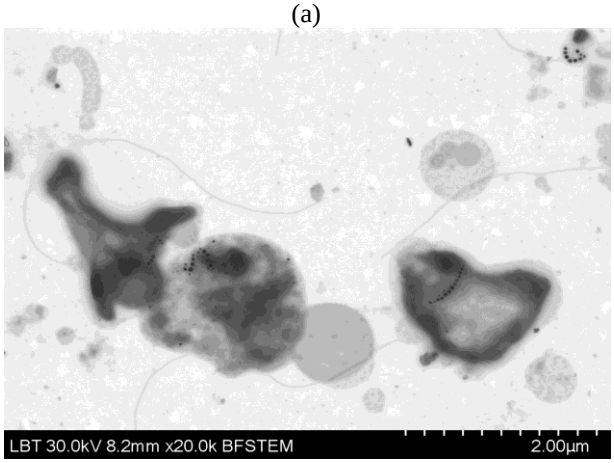

(c)

(d)

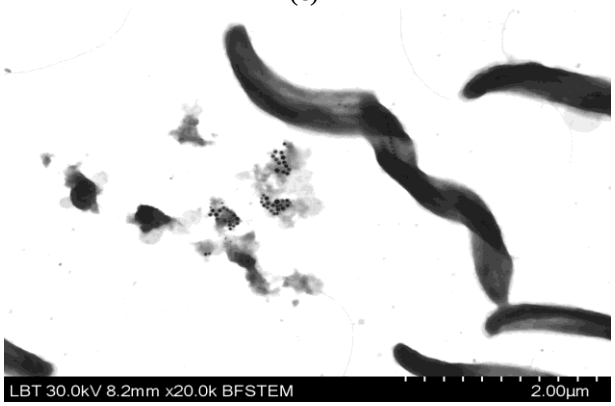

(e)

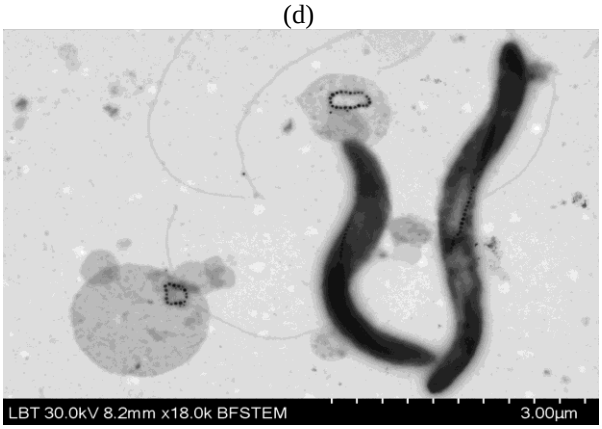

(f)

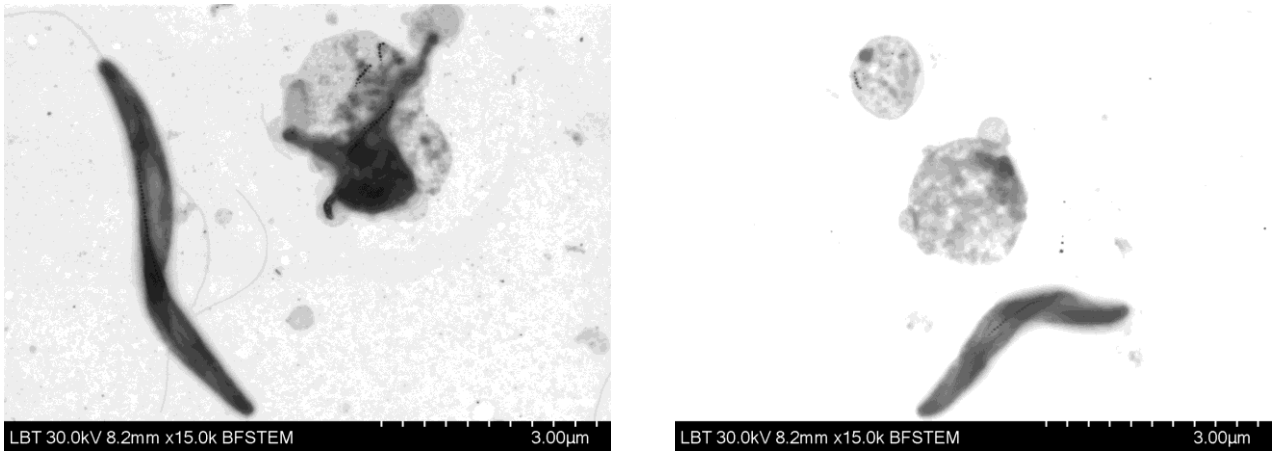

(g) (h)

Fig. 5 Images of cellular modifications of MTB cells after PMF treatments

ATR-FTIR Analysis of Spectra of the *Magnetospirillum gryphiswaldense* Cell Suspensions

The ATR-FTIR spectra are presented in Fig. 6. These spectra show clear differences between the control sample (black curve / superior trace) and the PMF exposed samples (coloured curves).

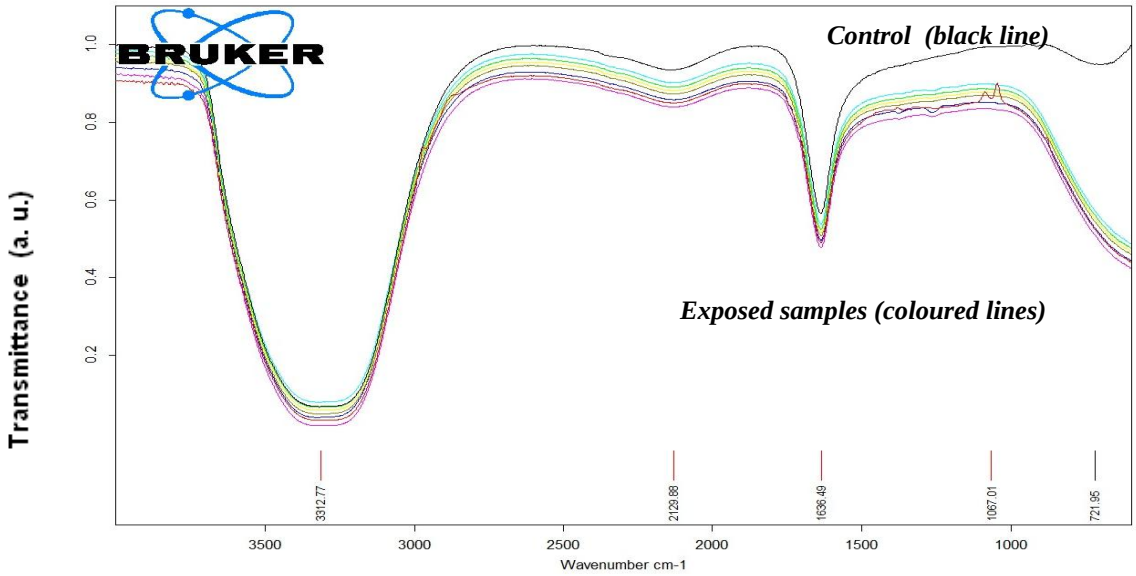

Fig. 6 ATR-FTIR spectra of the control and treated samples of MTB bacteria cells

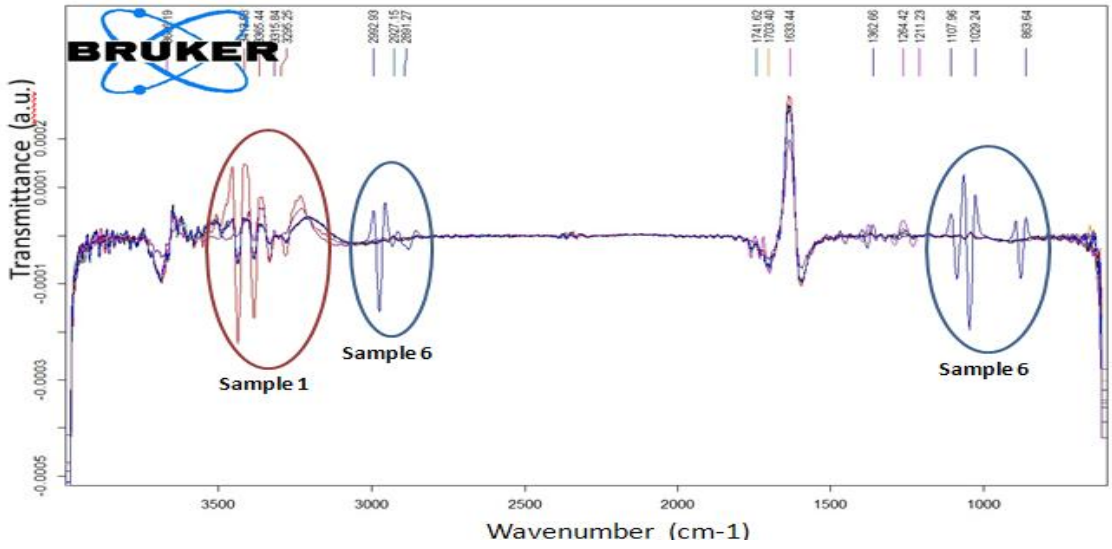

Fig. 7 ATR-FTIR second-derivative spectra of control and treated MTB cells samples

Our FTIR spectra are in good agreement with similar results reported in [26]. The presence of Fe-O bonds in the MS chains have be detected in all samples at values < 600 cm^{-1} embedded with amino N-H bending (1636.49 cm^{-1}), C-N stretching (1067-1250 cm^{-1}), amide C=O group (strong 1636.49 cm^{-1}) associated with N-H stretching at 3312.77 cm^{-1}. The strong broad band at 3312.77 cm^{-1} may also be attributed to stretching of O-H group present in magnetosome. Particularly in sample P1 there is a weak band at 1067.01 cm^{-1}, probably due to amine stretching. These peaks may be associated with proteins from bacterial cells. The broad peak at 2129.88 cm^{-1} can be assigned to stretching C≡N group. Because broad bands in original FTIR spectra may be attributed to overlapping of multi-component bands, the second-derivative spectra were performed and are presented in Fig. 7. In this figure, compared to control (untreated sample), an increase in the intensity of absorption bands in the region 2890-2992 cm^{-1} and 860-1110 cm^{-1} was registered in sample P1, and an increase of the absorption bands in the region of 3290-3420 cm^{-1} was observed in sample P6, according to different applied treatments (pulse trains versus bursts cycles). The observed changes in the region 3290-3420 cm^{-1} and 2890-2992 cm^{-1} might be associated to changes in the fatty acid profile of the samples, due to characteristic bands of C–H stretching vibrations of C≡C, C=C, and Ar–H (polyunsaturated fatty acids) and of CH_3 and CH_2 groups of lipids, respectively. These minute differences may reveal peculiar response to different time-frequency-amplitude distribution of the PMF stimuli.

CONCLUSION

A mild cellular integrity damaging, apparition of cyst-like cells (spheroplasts / coccoid cells, with or without magnetosome chains inside) and abnormal magnetosome chains were present with a low frequency of apparition in the magnetotactic bacteria live cells suspensions, after the pulsed magnetic field treatments with flux densities of maximum 125 mT and pulses of 400 μs duration. Overall, images of scanning-transmission electron microscopy did not reveal specificities connected to the type of magnetic stimuli (pulse trains or bursts cycles). Moreover, even in the control samples (not exposed), some abnormal cells could be visualised, but with very reduced frequency of apparition. However, the apparition of magnetosome chains in a loop shape was a very peculiar effect and may be connected to the modification of the magnetic dipole orientation of individual magnetosomes. Collapsing of magnetosome chains may be due to cytoskeleton (filaments) damage through modification in conformation of actin-like protein of these filaments, hypothesis in convergence with observations reported in [27].

Modifications of infrared spectra of magnetotactic bacteria suspensions due to pulsed magnetic field and minute differences between types of stimuli (trains or bursts) traced by the second derivative of the spectra show that some proteins may most probably be affected by the exposure. The results presented here are preliminary findings and future research will prove if the observed phenomena may be related to periodic variations of magnetic field strength.

REFERENCES

[1]. E Alphandery, Applications of magnetosomes synthesized by magnetotactic bacteria in medicine, *Frontiers in Bioengineering and Biotechnology*, 2014, 2, article ID 5.

[2]. S Barber-Zucker, N Keren-Khadmy, R Zarivach, From Invagination to Navigation: The Story of Magnetosome-Associated Proteins in Magnetotactic Bacteria, *Protein Science*, 2016, 25(2), 338-351.

[3]. AG Meyra, GJ Zarragoicoechea, VA Kuz, Magnetosome Chain Viewed As A Bio-Elastic Magnet, *Physical Chemistry Chemical Physics*, 2016, 18(18), 45-56

[4]. S Miclaus, P Bechet, G Mihai, C Moisescu, II Ardelean, L Barbu-Tudoran, TM Radu, S. Oancea, M Racuciu, Radiofrequency Stimuli Applied to Suspensions Containing Biogenic Magnetite Nanocrystals: Absorbed Energy Conversion, 10th *International Conference and Exposition on Electrical And Power Engineering (EPE)*, Iasi, Romania, 2018, 0143-0148.

[5]. I Orue, L Marcano, P Bender, A García-Prieto, S Valencia, MA Mawass, D Gil-Cartón, D Alba Venero, D Honecker, A García-Arribas, L Fernández Barquín, A Muela and M L Fdez-Gubieda, Configuration of the Magnetosome Chain: A Natural Magnetic Nanoarchitecture, *Nanoscale*, 2018, 10, article ID 7407.

[6]. M Blondeau, Y Guyodo, F Guyot, C Gatel, N Menguy, I Chebbi, B Haye, M Durand-Dubief, E Alphandery, R Brayner, T Coradin, Magnetic-Field Induced Rotation of Magnetosome Chains in Silicified Magnetotactic Bacteria, *Scientific Reports*, 2018, 8(1), article ID 7699

[7]. C Zahn, S Keller, M Toro-Nahuelpan, P Dorscht, W Gross, M Laumann, S Gekle, W Zimmermann, D Schüler, H Kress, Measurement of the Magnetic Moment of Single Magnetospirillum gryphiswaldense Cells by Magnetic Tweezers, *Scientific Reports*, 2017, 7, article ID 3558

[8]. A Körnig, J Dong, M Bennet, M Widdrat, J Andert, FD Müller, D Schüler, S Klumpp, D Faivre, Probing the Mechanical Properties of Magnetosome Chains in Living Magnetotactic Bacteria, *Nano Letters*, 2014, 14(8), 4653–4659.

[9]. W Pan, Effects of Pulsed Magnetic Field on The Formation of Magnetosomes in the Magnetospirillum Sp. Strain AMB-1, *Bioelectromagnetics*, 2010, 31, 246–251

[10]. X Wang, L Liang, T Song, L Wu, Magnetosome Formation and Expression of mamA, mms13, mms6 and magA in Magnetospirillum magneticum AMB-1 Exposed to Pulsed Magnetic Field, *Current Microbiology*, 2009, 59, 221–226
[11]. JC Diaz Ricci, BJ Woodford, JL Kirschvink, MR Hoffmann, Alteration of the Magnetic Properties of Aquaspirillum magnetotacticum by a Pulse Magnetization Technique, *Applied and Environmental Microbiology*, 1991, 57,11, 3248-3254
[12]. Y Meng, *Cellular Level Studies and Coil System Design for Transcranial Magnetic Stimulation*, Graduate Theses and Dissertations. 14511., Iowa State University Capstones, USA, https://lib.dr.iastate.edu/etd/14511, 2015.
[13]. S Miclaus, C Iftode and A Miclaus, Would the human brain be able to erect specific effects due to the magnetic field component of an UHF field via magnetite nanoparticles?, *Progress in Electromagnetic Research M*, 2018, 69, 23-36.
[14]. T Odutola, E Myrovali, A Makridis, N Maniotis, M Angelakeris, V Kimiskidis, T Samaras, Can Magnetic Nanoparticles Thermally Assist the Beneficiary Role of Transcranial Magnetic Stimulation?, *Proceedings of 1st World Conference on Biomedical Applications of Electromagnetic Fields (EMF-Med)*, Split, Croatia, 2018.
[15]. R Chen, G Romero, MG Christiansen, A Mohr, P Anikeeva, Wireless Magnetothermal Deep Brain Stimulation, *Science*, 2015, 347(6229), 1477-1480.
[16]. Z Shankayi, SM Firoozabadi, M Mansourian, A Mahna, The Effects of Pulsed Magnetic Field Exposure on the Permeability of Leukemia Cancer Cells, *Electromagnetic in Biology and Medicine*, 2014, 33(2),154-158.
[17]. M Soldati, M Mikkonen, I Laakso, T Murakami, Y Ugawa, A Hirata, A Multi-Scale Computational Approach Based on TMS Experiments for the Assessment of Electro-Stimulation Thresholds of the Brain at Intermediate Frequencies, *Physics in Medicine and Biology*, 2018, 63(22) , article ID 225006.
[18]. U Heyen, D Schüler, Growth and magnetosome formation by microaerophilic Magnetospirillum strains in an oxygen-controlled fermentor, *Applications in Microbiology and Biotechnology*, 2003, 61(5-6), 536-544.
[19]. F Faghihzadeh, NM Anaya, LA Schifman, V Oyanedel-Craver, Fourier Transform Infrared Spectroscopy to Assess Molecular-Level Changes in Microorganisms Exposed to Nanoparticles, *Nanotechnology and Environmental Engineering*, 2016, 1, paper no.1
[20]. Z Wei, D Jiao, J Xu, Using Fourier Transform Infrared Spectroscopy to Study Effects of Magnetic Field Treatment on Wheat (Triticum aestivum L.) Seedlings, *Journal of Spectroscopy*, 2015, article ID 570190
[21]. L Xiang, J Wei, S Jianbo, W Guili, G Feng and L Ying, Purified and Sterilized Magnetosomes from Magnetospirillum gryphiswaldense MSR-1 Were not Toxic to Mouse Fibroblasts in Vitro, *Letters in Applied Microbiology*, 2007, 45(1), 75-81.
[22]. JB Sun, JH Duan, SL Dai, J Ren, L Guo, W Jiang, Y Li, Preparation and Anti-Tumor Efficiency Evaluation of Doxorubicin-Loaded Bacterial Magnetosomes: Magnetic Nanoparticles as Drug Carriers Isolated from Magnetospirillum gryphiswaldense, *Biotechnology and Bioengineering*, 2008, 101(6), 1313-1320
[23]. T. Saranya, K. Parasuraman, M. Anbarasu, K Balamurugan, XRD, FT-IR and SEM Study of Magnetite (Fe_3O_4) Nanoparticles Prepared by Hydrothermal Method, *Nano Vision*, 2015, 5(4-6), 149-154
[24]. DL Balkwill, D. Maratea, RP Blakemore, Ultrastructure of a Magnetotactic Spirillum, *Journal of Bacteriology*, 1980, 141, 3, 1399-1408
[25]. SA Lyshevski, *Nano- and Micro-Electromechanical Systems: Fundamentals of Nano- and Microengineering*, 2nd ed., CRC Press, New York, p. 276, 2005.
[26]. T. Revathy, MA Jayasri, K Suthindhiran, Toxicity Assessment of Magnetosomes in Different Models, *Biotechnology*, 2017, 7, paper no. 126.
[27]. E Katzmann, A Scheffel, M Gruska, JM Plitzko, D Schüler, Loss of the Actin-Like Protein MamK has Pleiotropic Effects on Magnetosome Formation and Chain Assembly in Magnetospirillum gryphiswaldense, *Molecular Microbiology*, 2010, 77(1), 208-224.